

Lyapunov-Based Deep Neural Networks for Adaptive Control of Stochastic Nonlinear Systems

Saiedeh Akbari, Cristian F. Nino, Omkar Sudhir Patil, Warren E. Dixon*

Abstract—Controlling nonlinear stochastic dynamical systems involves substantial challenges when the dynamics contain unknown and unstructured nonlinear state-dependent terms. For such complex systems, deep neural networks can serve as powerful black box approximators for the unknown drift and diffusion processes. Recent developments construct Lyapunov-based deep neural network (Lb-DNN) controllers to compensate for deterministic uncertainties using adaptive weight update laws derived from a Lyapunov-based analysis based on insights from the compositional structure of the DNN architecture. However, these Lb-DNN controllers do not account for non-deterministic uncertainties. This paper develops Lb-DNNs to adaptively compensate for both the drift and diffusion uncertainties of nonlinear stochastic dynamic systems. Through a Lyapunov-based stability analysis, a DNN-based approximation and corresponding DNN weight adaptation laws are constructed to eliminate the unknown state-dependent terms resulting from the nonlinear diffusion and drift processes. The tracking error is shown to be uniformly ultimately bounded in probability. Simulations are performed on a nonlinear stochastic dynamical system to show efficacy of the proposed method.

Index Terms—Stochastic systems, Lyapunov methods, deep neural networks, adaptive control, nonlinear control systems

I. INTRODUCTION

Stochastic control theory has received considerable attention, due to its far-reaching applicability across various domains [1]–[6]. Modeling the uncertainty in the system as a stochastic process can make the control design less conservative than assuming the worst-case upper bounds of the uncertainty [7]. However, due to the stochastic nature of such systems, many challenges are introduced in designing an adaptive controller for such systems.

To illustrate the challenges involved in designing an adaptive controller for stochastic systems, consider a nonlinear stochastic system of the form

$$dx = F(x, u) dt + G(x, t) d\omega, \quad (1)$$

where x denotes the state, F denotes the drift process, and G denotes the diffusion process. For many practical systems, the drift and diffusion processes may be expressed in a control-affine form given by $F(x, u) \triangleq f(x) + g_1(x)u$ and $G(x, t) \triangleq g_2(x)\Sigma(t)$, where f , g_1 , and u respectively denote to drift vector field, control effectiveness, and the control input, and

g_2 is a matrix-valued diffusion function and Σ is a nonnegative matrix-valued function. To address the control problem for systems modeled as (1), early works in the literature assume model knowledge of F and G (e.g., [1], [2]). Although several results compensate for drift uncertainties, fewer works pay attention to compensating for diffusion uncertainties.

To compensate for the drift and diffusion uncertainties, different robust and adaptive compensation approaches have been developed (e.g., [8]–[15]). Shallow NNs are often used to compensate for uncertainties in nonlinear stochastic systems due to their inherent function approximation capabilities, to fulfill either stabilization or trajectory tracking objectives (e.g., [12], [15]–[20]). Despite considerable advances, controlling nonlinear stochastic systems involves enduring.

- Assumption of known sign/value of bounds or known structure of the uncertainties: In results such as [18] and [19], the NN is only used to approximate $f(x)$, whereas $g_2(x)$ is upper bounded. Additionally, in results such as [15] and [20], diffusion and drift uncertainties are assumed have a known linear-in-parameter structure, where the unknown parameters are estimated using an adaptive approach. For example, [12] requires a bound with known sign on the drift vector. In this paper, assumptions on structure of the drift and diffusion uncertainties and any knowledge on the value or sign of their bounds are avoided.
- No probabilistic analysis for the escape risk: Studies such as [12], [16]–[19] do not provide probabilistic analysis to account for the risk of the states escaping from the compact set, where the universal function approximation property is guaranteed to hold. For stochastic dynamics, there is a probability of solutions escaping the compact set, even when initialized within the compact set [21, Chap. 3]. Even for deterministic systems, the state trajectories need to be shown to lie in a compact set by appropriately shaping the set [22, Def. 4.6]. A unique contribution of this paper is a lemma that expresses the probability of escape in terms of the ultimate bound and the initial condition of the Lyapunov function.
- Vanishing stochastic noise: A key assumption across studies with global asymptotic stable (GAS) results (such as [1], [2]) and uniformly ultimately bounded (UUB) results (such as [6], [12], [15], [17], [18], [20]), is that the equilibrium is preserved under the presence of the noise, i.e., $g_2(0) = 0$. This assumption is conservative since it implies that once perfect tracking is achieved and the system is at equilibrium, the stochastic noise disappears. Such an assumption is not applicable to most

*Saiedeh Akbari, Cristian F. Nino, Omkar Sudhir Patil, and Warren E. Dixon are with the department of Mechanical Engineering and Aerospace Engineering, University of Florida, Gainesville, FL, 32611-6250 USA. Email: {akbaris, cristian1928, patilomkarsudhir, wdixon}@ufl.edu.

This research is supported in part by AFOSR grant FA9550-19-1-0169. Any opinions, findings, and conclusions or recommendations expressed in this material are those of the author(s) and do not necessarily reflect the views of the sponsoring agencies.

real-world applications and is avoided in this paper. Furthermore, a correlation between the noise at the origin and the ultimate bound is shown that offers an insightful examination of the escape risk.

Deep neural networks (DNNs) leverage the nested nonlinearities arising from function composition, resulting in enhanced function approximation performance even with fewer overall parameters when compared to a corresponding shallow NN, as evidenced by empirical and experimental findings [23]–[25]. Most existing DNN results use offline training by using sampled input-output datasets (e.g., [26, Sec. 6.6] and [27]–[29]). The aforementioned DNNs are applied as feedforward terms, and once implemented, the weights of the DNNs cannot be updated in real-time via a Lyapunov stability driven update law. Hence, this open-loop implementation lacks stability guarantees. Recent breakthroughs address the lack of stability and adaptation to unexpected uncertainties by introducing Lyapunov-based DNNs (Lb-DNN) which use Lyapunov-based techniques to update the weights of the DNN in real-time [30]–[34]. Specifically, the weights of Lb-DNNs are adjusted from analytic update laws designed from a Lyapunov-based stability analysis, allowing for real-time weight updates of the DNN without requiring pre-training from offline data [30], [31]. To the best of the authors’ knowledge, the result in [35] is only one result that employs Lb-DNNs for control of nonlinear stochastic systems. In [35], Lb-DNNs are used for an optimized backstepping control design in a class of stochastic nonlinear strict-feedback systems. However, the probability of solutions escaping the compact set is not considered and the assumption of noise vanishing at the equilibrium is made.

In this paper, the trajectory tracking problem is addressed for a general class of control-affine nonlinear stochastic dynamical systems with unstructured uncertainties. To allow for targeted adjustments for each uncertain component (i.e., terms stemming from $f(x)$, $g(x)$, and $\Sigma(t)$), the developed method uses three Lb-DNNs to approximate the inherent deterministic and stochastic uncertainties within the closed-loop error system.¹ The main contributions of this paper are summarized as below.

- 1) Lb-DNNs are utilized to compensate for the uncertainties of a nonlinear stochastic dynamical system. By taking advantage of the superior function approximation capabilities of DNNs and improved performance of the Lb-DNNs compared to shallow NNs [30], a multi-DNN technique is developed such that three different Lb-DNNs individually approximate components stemming from drift and diffusion uncertainties.
- 2) The assumption of vanishing noise is relaxed by a strategic use of Taylor’s theorem and properties of the trace operator in the subsequent stability analysis. Relaxing this assumption allows for non-vanishing noise, which adds to the challenges in the stability analysis, but makes the developed method better suited for real-world applications. Furthermore, an additional generality is added

¹One DNN architecture may also be used instead of three to compensate for the uncertainties, however, using multiple DNNs allows for targeted adjustments.

that the noise has an unknown time-varying covariance matrix that is multiplied by the nonlinearity of the diffusion matrix. Additionally, there are no assumptions on the structure of the uncertainties. Moreover, any assumption regarding knowledge on the uncertainties or the sign and value of their upper-bounds are relaxed compared to the literature.

- 3) A Lyapunov-based stability analysis is conducted to guarantee probabilistic exponential convergence to an ultimate bound about the origin and the boundedness of all the signals. Through the stability analysis, the tracking error is shown to be uniformly ultimately bounded in probability and a theorem is developed to quantify the probability of stability. For the universal approximation property to hold, all states that are inputs to the DNN must be constrained to a compact set, for all time. Due to the stochastic nature of the dynamics, the stability result is proven in probability, meaning that there is a risk that states may escape the aforementioned compact set. From a practical perspective, quantifying the escape risk is essential to provide a probabilistic certification on the designed controller. Hence, it is crucial to quantify this risk via a probability analysis. Although for asymptotically stable results, a probability analysis is typically provided (see [1], [15], [20]), for results with uniform ultimate bounds in probability, a probability analysis is usually not provided.

Simulations are performed on a five-dimensional nonlinear stochastic dynamical system to show the efficacy of the proposed method. Additional simulations illustrate the tracking performance of the proposed controller in response to variations in mean and covariance of the stochastic noise.

II. NOTATION

Let $\mathbf{0}_{m \times n}$ and $I_{m \times n}$ denote the $m \times n$ dimensional zero and identity matrices, respectively. The universal quantifier $\forall \varpi(x)$ asserts that $\varpi(x)$ is true for every x in the domain. The existential quantifier $\exists x \varpi(x)$ asserts that $\varpi(x)$ is true for at least one x in the domain. Implication $\varpi \implies \varphi$ is defined as $\neg \varpi \vee \varphi$, where negation $\neg \varpi$ means ϖ is false, and disjunction $\varpi \vee \varphi$ means at least one of ϖ or φ is true. The colon symbol $:$ in set-builder notation, as in $\{x : \varpi(x)\}$, means “such that” and specifies the element x in the domain for which the condition $\varpi(x)$ holds. The right pseudo inverse of a full-row-rank matrix A is defined as $A^+ (\cdot) \triangleq A^\top (\cdot) (A (\cdot) A^\top (\cdot))^{-1}$. The expected value is given by $E[X] = \int_{-\infty}^{\infty} x \cdot \mathbf{F}(x) dx$, where $\mathbf{F}(x)$ is the probability density function of the continuous random variable X . For a matrix $A \triangleq [a_{i,j}] \in \mathbb{R}^{n \times m}$, where $a_{i,j}$ is the element on the i^{th} row of the j^{th} column of the matrix, the vectorization operator is defined as $\text{vec}(A) = [a_{1,1}, \dots, a_{n,1}, \dots, a_{1,m}, \dots, a_{n,m}]^\top \in \mathbb{R}^{nm}$. For a square matrix $A \in \mathbb{R}^{n \times n}$, the trace operator is defined as $\text{tr}(A) = \sum_{i=1}^n a_{i,i}$, where $a_{i,i}$ represents the element on the i^{th} row of the i^{th} column. From [36, Chapter 2, Eq. 13], the trace to vector property

$$\text{tr}(A^\top B) = \text{vec}(A)^\top \text{vec}(B) \quad (2)$$

holds for matrices A and B . From [36, Chapter 1, Eq. 25],

$$\text{tr}(ABC) = \text{tr}(BCA) = \text{tr}(CAB). \quad (3)$$

Additionally, if A and B are positive semi-definite matrices, then

$$\text{tr}(AB) \leq \text{tr}(A) \text{tr}(B). \quad (4)$$

The right-to-left matrix product operator is represented by $\widehat{\prod}$, i.e., $\widehat{\prod}_{p=1}^m A_p = A_m \dots A_2 A_1$ and $\widehat{\prod}_{p=a}^m A_p = I$ if $a > m$. The Kronecker product is denoted by \otimes . From [31] and given any $A \in \mathbb{R}^{p \times a}$, $B \in \mathbb{R}^{a \times r}$, and $C \in \mathbb{R}^{r \times s}$, differentiating $\text{vec}(ABC)$ on both sides with respect to $\text{vec}(B)$ yields

$$\frac{\partial}{\partial \text{vec}(B)} \text{vec}(ABC) = C^\top \otimes A. \quad (5)$$

Given a function $h : \mathbb{R}^n \rightarrow \mathbb{R}^n$, the notation $\lim_{a \rightarrow b^-} h(a)$ denotes the left-hand limit of h at b . The p -norm is denoted by $\|\cdot\|_p$, where the subscript is suppressed when $p = 2$. The Frobenius norm is denoted by $\|\cdot\|_F \triangleq \|\text{vec}(\cdot)\|$. For a bounded function $f : \mathbb{R}_{\geq 0} \rightarrow \mathbb{R}^{n \times m}$, $\|f\|_{F\infty} \triangleq \sup_{t \in \mathbb{R}_{\geq 0}} \|f\|_F$. The space

of k -times differentiable functions is denoted by \mathcal{C}^k , and a \mathcal{C}^∞ -smooth function is an infinitely differentiable function. For $A \subseteq \mathbb{R}^n$ and $B \subseteq \mathbb{R}^m$, let $C(A, B)$ denote the set of continuous functions $f : A \rightarrow \mathbb{R}^m$ such that $f(A) \subseteq B$, and let $C(A) \triangleq C(A, A)$. In the filtered probability space of $(\Omega, \mathbb{F}, \mathbb{F}_t, P)$, Ω represents the event space, \mathbb{F} denotes a σ -algebra of the subsets of Ω and represents the event space, \mathbb{F}_t is a complete filtration given by the family of σ -algebras up to time t , i.e., $\mathbb{F}_S : \mathbb{F}_S \subseteq \mathbb{F}_t \forall t \in [0, t]$, and P is a probability measure, where the filtration is complete in the sense it includes all events with probability measure zero (see [37]). Consider a probability space of (Ω, \mathbb{F}, P) . Then, for any events $A, B \in \mathbb{F}$ such that $A \subseteq B$, the monotonicity property states that [38, eq. 2.5]

$$P(A) \leq P(B). \quad (6)$$

Consider the dynamical system in (1). Then, for some function $V \in \mathcal{C}^2$ associated with the process in (1), let the infinitesimal generator \mathcal{L} of the function $V(x)$ be defined as [39, eq. 4.12]

$$\mathcal{L}V \triangleq \frac{\partial V}{\partial x} f(x) + \frac{1}{2} \text{tr} \left(G(x, t)^\top \frac{\partial^2 V}{\partial x^2} G(x, t) \right). \quad (7)$$

A. Deep Neural Network Model

Let $\kappa \in \mathbb{R}^{L_0}$ denote the DNN input, and $\theta \in \mathbb{R}^p$ denote the vector of DNN parameters (i.e., weights and bias terms). A fully-connected feedforward DNN $\Phi(\kappa, \theta)$ with $k \in \mathbb{Z}_{>0}$ hidden layers and output size $L_{k+1} \in \mathbb{Z}_{>0}$ is defined using a recursive relation $\varphi_j \in \mathbb{R}^{L_{j+1}}$ modeled as

$$\varphi_j \triangleq \begin{cases} V_{j+1}^\top \kappa_a, & j = 0, \\ V_{j+1}^\top \phi_j(\varphi_{j-1}) & j \in \{1, \dots, k\}, \end{cases} \quad (8)$$

where $\Phi(\kappa, \theta) = \varphi_k$, $\kappa_a \triangleq [\kappa^\top, 1]^\top$ denotes the augmented input that accounts for the bias terms, $L_j \in \mathbb{Z}_{>0}$ denotes the number of neurons in the j^{th} layer with $L_j^a \triangleq L_j + 1$, and

$V_{j+1} \in \mathbb{R}^{L_j^a \times L_{j+1}}$ denotes the matrix of weights and biases, for all $j \in \{0, \dots, k\}$.

The vector of activation functions is denoted by $\phi_j : \mathbb{R}^{L_j} \rightarrow \mathbb{R}^{L_j^a}$ for all $j \in \{1, \dots, k\}$. The vector of activation functions can be composed of various activation functions, and hence, may be represented as $\phi_j = [\varsigma_1, \dots, \varsigma_{L_j}, 1]^\top$ for all $j \in \{1, \dots, k\}$, where $\varsigma_j : \mathbb{R} \rightarrow \mathbb{R}$ for all $j \in \{1, \dots, L_j\}$ denotes a piece-wise continuously differentiable activation function, where 1 denotes the augmented hidden layer that accounts for the bias terms. For the DNN architecture in (8), the vector of DNN weights is $\theta \triangleq [\text{vec}(V_1)^\top, \dots, \text{vec}(V_k)^\top]^\top$ with size $p = \sum_{j=0}^k L_j^a L_{j+1}$.

Consider $y_j \in \mathbb{R}^{L_j}$ where $y_j = [y_1, \dots, y_{L_j}]$ with $y_i \in \mathbb{R}$ for all $i \in \{1, \dots, L_j\}$. The Jacobian $\frac{\partial \phi_j}{\partial y_j} : \mathbb{R}^{L_j} \rightarrow \mathbb{R}^{L_j^a \times L_j}$ of the activation function vector at the j^{th} layer is given by $[\varsigma'_1(y_1)\eta_1, \dots, \varsigma'_{L_j}(y_{L_j})\eta_{L_j}, \mathbf{0}_{L_j}]^\top \in \mathbb{R}^{L_j^a \times L_j}$, where ς'_j denotes the derivative of ς_j with respect to its argument for $j \in \{1, \dots, L_j\}$, η_i is the i^{th} standard basis vector in \mathbb{R}^{L_j} , and $\mathbf{0}_{L_j}$ is the zero vector in \mathbb{R}^{L_j} .

Let the gradient of the DNN with respect to the weights be denoted by $\Phi'(\kappa, \theta) \triangleq \frac{\partial}{\partial \theta} \Phi(\kappa, \theta)$, which can be represented as $\Phi'(\kappa, \theta) = \left[\frac{\partial}{\partial \text{vec}(V_1)} \Phi(\kappa, \theta), \dots, \frac{\partial}{\partial \text{vec}(V_k)} \Phi(\kappa, \theta) \right] \in \mathbb{R}^{L_{k+1} \times p}$, where $\frac{\partial}{\partial \text{vec}(V_j)} \Phi(\kappa, \theta) \in \mathbb{R}^{L_{k+1} \times L_j^a L_j}$ for all $j \in \{1, \dots, k+1\}$. Then, using (8) and the property of the vectorization operator in (5) yields

$$\Phi'(\kappa, \theta) = \left(\widehat{\prod}_{\ell=j+1}^k V_{\ell+1}^\top \frac{\partial \phi_\ell}{\partial \varphi_{\ell-1}} \right) (I_{L_{j+1}} \otimes \varrho_j), \quad (9)$$

for $j \in \{0, \dots, k\}$, where $\varrho_j = \kappa_a^\top$ if $j = 0$ and $\varrho_j = \phi_j^\top(\varphi_{j-1})$ if $j \in \{1, \dots, k\}$.

III. DYNAMICS AND CONTROL OBJECTIVE

Consider a stochastic process modeled by the control-affine nonlinear stochastic differential equation

$$dx = (f(x) + g_1(x)u(t))dt + g_2(x)\Sigma(t)d\omega, \quad (10)$$

where $t \in \mathbb{R}_{\geq 0}$ denotes time, $x \in \mathbb{R}^n$ denotes the known state variable, $f : \mathbb{R}^n \rightarrow \mathbb{R}^n$ denotes an unknown continuous drift vector field, $g_1 : \mathbb{R}^n \rightarrow \mathbb{R}^{n \times r}$ denotes the known control effectiveness matrix, and $u \in \mathbb{R}^r$ denotes the control input. Additionally, in (10), $g_2 : \mathbb{R}^n \rightarrow \mathbb{R}^{n \times s}$ denotes the continuous diffusion matrix, $\Sigma : \mathbb{R}_{\geq 0} \rightarrow \mathbb{R}^{s \times s}$ denotes the symmetric Borel measurable covariance matrix, and $\omega \in \mathbb{R}^s$ denotes the s -dimensional independent standard Wiener process defined on the complete filtered probability space $(\Omega, \mathbb{F}, \mathbb{F}_t, P)$, respectively.

Assumption 1. The control effectiveness matrix, g_1 , is full row rank, and bounded.

The objective of this paper is to design a controller such that the state x converges (in expectation) to a \mathcal{C}^2 -smooth user-defined desired trajectory $x_d : \mathbb{R}_{\geq 0} \rightarrow \mathbb{R}^n$. To quantify the control objective, the tracking error $e \in \mathbb{R}^n$ is defined as

$$e \triangleq x - x_d. \quad (11)$$

Assumption 2. There exist known constants $\overline{x_d}, \overline{\dot{x}_d} \in \mathbb{R}_{>0}$ such that $\|x_d\| \leq \overline{x_d}$ and $\|\dot{x}_d\| \leq \overline{\dot{x}_d}$.

To adapt to the uncertainties caused by the diffusion matrix in the subsequent stability analysis, Taylor's theorem is applied to the vectorized diffusion matrix g_2 , yielding

$$\text{vec}(g_2(x)) = \Psi(e, x_d)e + \text{vec}(g_2(x_d)), \quad (12)$$

where $\Psi: \mathbb{R}^n \times \mathbb{R}^n \rightarrow \mathbb{R}^{nm \times n}$ is a C^∞ -smooth function, and $\text{vec}(g_2(x_d))$ is upper-bounded as $\|\text{vec}(g_2(x_d))\| \leq \bar{g}$, where $\bar{g} \in \mathbb{R}_{>0}$ is unknown.

IV. CONTROL DESIGN

As previously discussed, the multi-DNN architecture in the subsequent control development allows for targeted adjustments to individual uncertain components. Let $\mathbf{x} \triangleq [x^\top, x_d^\top]^\top \in \mathbb{R}^{2n}$. The terms $\mathcal{F}_1: \mathbb{R}^n \rightarrow \mathbb{R}$, and $\mathcal{F}_2: \mathbb{R}^{2n} \rightarrow \mathbb{R}^n$ are introduced based on the subsequent analysis and are defined as $\mathcal{F}_1(x) \triangleq \|\Sigma\|_{F^\infty}^2 \text{tr}(\Psi(x)^\top \Psi(x))$ and $\mathcal{F}_2(\mathbf{x}) \triangleq \|\Sigma\|_{F^\infty}^2 \Psi(x)^\top \text{vec}(g_2(x_d))$, respectively. Leveraging the universal function approximation properties offered by DNNs, three separate Lb-DNNs are developed to approximate f , \mathcal{F}_1 , and \mathcal{F}_2 .

A. Deep Neural Network Architecture

Define the compact domains

$$\begin{aligned} \Omega_1 &\triangleq \{\zeta \in \mathbb{R}^n : \|\zeta\| \leq \chi + \overline{x_d}\}, \\ \Omega_2 &\triangleq \{\xi \in \mathbb{R}^{2n} : \|\xi\| \leq \chi + 2\overline{x_d}\}, \end{aligned} \quad (13)$$

where $\chi \in \mathbb{R}_{>0}$ denotes a bounding constant. Prescribe $\bar{\varepsilon}_\ell \in \mathbb{R}$, and note that $f \in C(\Omega_1, \mathbb{R}^n)$, $\mathcal{F}_1 \in C(\Omega_1, \mathbb{R})$, and $\mathcal{F}_2 \in C(\Omega_2, \mathbb{R}^{2n})$, for all $t \in \mathbb{R}_{\geq 0}$ and $\ell \in \{1, 2, 3\}$. By [40, Thm. 3.2], there exist Lb-DNNs such that $\sup_{x \in \Omega_1} \|\Phi_1(x, \theta_1^*) - f(x)\| \leq \bar{\varepsilon}_1$, $\sup_{x \in \Omega_1} \|\Phi_2(x, \theta_2^*) - \mathcal{F}_1(x)\| \leq \bar{\varepsilon}_2$, and $\sup_{\mathbf{x} \in \Omega_2} \|\Phi_3(\mathbf{x}, \theta_3^*) - \mathcal{F}_2(\mathbf{x})\| \leq \bar{\varepsilon}_3$. Therefore, the uncertainties can be modeled using three separate Lb-DNNs as

$$f(x) = \Phi_1(x, \theta_1^*) + \varepsilon_1(x), \quad (14)$$

$$\mathcal{F}_1(x) = \Phi_2(x, \theta_2^*) + \varepsilon_2(x), \quad (15)$$

$$\mathcal{F}_2(\mathbf{x}) = \Phi_3(\mathbf{x}, \theta_3^*) + \varepsilon_3(\mathbf{x}), \quad (16)$$

for all $x \in \Omega_1$ and $\mathbf{x} \in \Omega_2$, where $\Phi_1: \mathbb{R}^n \times \mathbb{R}^{p_1} \rightarrow \mathbb{R}^n$, $\Phi_2: \mathbb{R}^n \times \mathbb{R}^{p_2} \rightarrow \mathbb{R}$, $\Phi_3: \mathbb{R}^{2n} \times \mathbb{R}^{p_3} \rightarrow \mathbb{R}^n$, and $\varepsilon_1: \mathbb{R}^n \rightarrow \mathbb{R}^n$, $\varepsilon_2: \mathbb{R}^n \rightarrow \mathbb{R}$, and $\varepsilon_3: \mathbb{R}^{2n} \rightarrow \mathbb{R}^n$ denote the unknown function reconstruction errors that can be bounded as $\sup_{x \in \Omega_1} \|\varepsilon_1(x)\| \leq \bar{\varepsilon}_1$, $\sup_{x \in \Omega_1} \|\varepsilon_2(x)\| \leq \bar{\varepsilon}_2$, and $\sup_{\mathbf{x} \in \Omega_2} \|\varepsilon_3(\mathbf{x})\| \leq \bar{\varepsilon}_3$. The following standard assumption is made to aid in the subsequent development (cf., [41, Assumption 1]).

Assumption 3. For all $\ell \in \{1, 2, 3\}$, the vector of ideal weights can be bounded as $\|\theta_\ell^*\| \leq \bar{\theta}_\ell$, where $\bar{\theta}_\ell \in \mathbb{R}_{>0}$ is a known bound. For cases where $\bar{\theta}_\ell$ is unknown, results such as [42] can be used to compensate for θ_ℓ .

B. Adaptive Update Law

Let $\hat{\theta}_\ell$ denote the adaptive estimates of the ideal weights θ_ℓ^* for all $\ell \in \{1, 2, 3\}$, and let the corresponding weight estimation errors be defined as

$$\tilde{\theta}_\ell \triangleq \theta_\ell^* - \hat{\theta}_\ell, \quad \forall \ell \in \{1, 2, 3\}. \quad (17)$$

Motivated by the subsequent Lyapunov-based stability analysis, the weight estimates are updated according to

$$\dot{\hat{\theta}}_1 \triangleq \text{proj}\left(\gamma_1 \Phi_1'^\top(x, \hat{\theta}_1)e - \gamma_1 \sigma_1 \hat{\theta}_1\right), \quad (18)$$

$$\dot{\hat{\theta}}_2 \triangleq \text{proj}\left(\frac{1}{2} \gamma_2 e^\top e \Phi_2'^\top(x, \hat{\theta}_2) - \gamma_2 \sigma_2 \hat{\theta}_2\right), \quad (19)$$

$$\dot{\hat{\theta}}_3 \triangleq \text{proj}\left(\gamma_3 \Phi_3'^\top(\mathbf{x}, \hat{\theta}_3)e - \gamma_3 \sigma_3 \hat{\theta}_3\right), \quad (20)$$

where $\gamma_\ell \in \mathbb{R}_{>0}$ denote user-defined learning rates, $\sigma_\ell \in \mathbb{R}_{>0}$ denote user-defined forgetting factors, and $\text{proj}(\cdot)$ denotes the smooth projection operator defined in [43, eq. (7)-(11)], which is used to ensure that $\hat{\theta}_\ell$ is bounded as $\hat{\theta}_\ell \leq \bar{\theta}_\ell$, for all $\ell \in \{1, 2, 3\}$.

To facilitate the subsequent stability analysis, a first-order Taylor approximation [31], [41, Eq. 22] is used on $\Phi_\ell - \hat{\Phi}_\ell$ to yield

$$\Phi_\ell - \hat{\Phi}_\ell = \hat{\Phi}_\ell' \tilde{\theta}_\ell + \mathcal{O}_l\left(\|\tilde{\theta}_\ell\|^2\right), \quad \forall \ell \in \{1, 2, 3\}. \quad (21)$$

By Assumption 3, boundedness of $\hat{\theta}_\ell$, and given bounded x , there exist constants $\Delta_\ell \in \mathbb{R}_{>0}$ such that $\left\|\mathcal{O}_l\left(\|\tilde{\theta}_\ell\|^2\right)\right\| \leq \Delta_\ell$, for all $\ell \in \{1, 2, 3\}$.

C. Controller and Closed-Loop Error System

To compensate for the uncertainties that appear in the subsequent closed-loop error system, the Lb-DNNs are incorporated into the developed controller, designed as

$$u(t) \triangleq g_1(x)^+ \left(\dot{x}_d - k_e e - \Phi_1(x, \hat{\theta}_1) - \frac{1}{2} e \Phi_2(x, \hat{\theta}_2) - \Phi_3(\mathbf{x}, \hat{\theta}_3) \right), \quad (22)$$

where $k_e \in \mathbb{R}_{>0}$ is a user-defined gain, and g_1^+ exists by Assumption 1 and [44]. Let $z: \mathbb{R}_{\geq 0} \rightarrow \mathbb{R}^\varphi$ denote the concatenated error state defined as $z \triangleq [e^\top, \tilde{\theta}_1^\top, \tilde{\theta}_2^\top, \tilde{\theta}_3^\top]^\top$,

where $\varphi \triangleq n + \sum_{\ell=1}^3 p_\ell$. Using (11), (17), and the chain rule,

dz is obtained as $dz = \left[dx - \frac{dx_d}{dt} dt, \frac{d\tilde{\theta}_1}{dt} dt, \frac{d\tilde{\theta}_2}{dt} dt, \frac{d\tilde{\theta}_3}{dt} dt \right]$. Substituting (10), (18)-(22) into dz yields the closed-loop error system

$$dz = F(z) dt + G(z, t) d\omega, \quad (23)$$

where $G(z, t) \triangleq [g_2(x) \Sigma(t), \mathbf{0}_{(\varphi-n) \times m}]^\top$ and

$$F(z) \triangleq \begin{bmatrix} f(x) - k_e e - \Phi_1(x, \hat{\theta}_1) - \frac{1}{2} e \Phi_2(x, \hat{\theta}_2) - \Phi_3(\mathbf{x}, \hat{\theta}_3) \\ -\text{proj}\left(\gamma_1 \Phi_1'^\top(x, \hat{\theta}_1)e - \gamma_1 \sigma_1 \hat{\theta}_1\right) \\ -\text{proj}\left(\frac{1}{2} \gamma_2 e^\top e \Phi_2'^\top(x, \hat{\theta}_2) - \gamma_2 \sigma_2 \hat{\theta}_2\right) \\ -\text{proj}\left(\gamma_3 \Phi_3'^\top(\mathbf{x}, \hat{\theta}_3)e - \gamma_3 \sigma_3 \hat{\theta}_3\right) \end{bmatrix}.$$

V. STABILITY ANALYSIS

Let $\mathcal{D} \triangleq \{\iota \in \mathbb{R}^\varphi : \|\iota\| \leq \chi\}$, where χ is previously introduced in (13), and consider the Lyapunov function candidate $V_L : \mathcal{D} \rightarrow \mathbb{R}_{\geq 0}$ defined as

$$V_L(z) \triangleq \frac{1}{2} e^\top e + \frac{1}{2} \bar{\theta}_1^\top \gamma_1^{-1} \bar{\theta}_1 + \frac{1}{2} \bar{\theta}_2^\top \gamma_2^{-1} \bar{\theta}_2 + \frac{1}{2} \bar{\theta}_3^\top \gamma_3^{-1} \bar{\theta}_3. \quad (24)$$

The Lyapunov function candidate can be bounded as

$$\alpha_1 \|z\|^2 \leq V_L(z) \leq \alpha_2 \|z\|^2, \quad (25)$$

where $\alpha_1 \triangleq \frac{1}{2} \min(1, \gamma_1^{-1}, \gamma_2^{-1}, \gamma_3^{-1})$ and $\alpha_2 \triangleq \max(1, \gamma_1^{-1}, \gamma_2^{-1}, \gamma_3^{-1})$.

The following definition is provided to assist with the subsequent stability analysis.

Definition 1. (Uniformly ultimately bounded in probability (UUB-p)) The solutions of (23) are uniformly ultimately bounded in probability with bound $b \in \mathbb{R}_{>0}$ and escape risk $e \in (0, 1)$, if there exists $c \in \mathbb{R}_{>0}$, independent of $t_0 \geq 0$, such that for every $a \in (0, c)$, there is $T = T(a, b) \geq 0$, independent of t_0 , such that

$$\|z(t_0)\| \leq a \Rightarrow \mathbb{P} \left(\sup_{0 \leq t \leq \infty} \|z(t)\| \geq b \right) \leq e, \quad \forall t \geq t_0 + T.$$

Based on the subsequent stability analysis, let the set of stabilizing initial conditions be defined as

$$\mathcal{S} \triangleq \left\{ \iota \in \mathbb{R}^\varphi : \|\iota\| \leq \sqrt{\frac{1}{\alpha_2} \sqrt{\frac{\alpha_1}{\alpha_2} \chi^2 - \frac{b}{c}}} \right\}. \quad (26)$$

The set to which all trajectories converge be defined as

$$\mathcal{B} \triangleq \left\{ \zeta \in \mathbb{R}^\varphi : \|\zeta\| \leq \sqrt{\frac{\lambda}{\alpha_1}} \right\}, \quad (27)$$

where $\lambda \in \left[\frac{b}{c}, m \right]$, $b \triangleq \frac{1}{2} (\Delta_1 + \Delta_3)^2 + \frac{1}{2} \|\Sigma \Sigma^\top\|_\infty \bar{g}^2 + \frac{\sigma_1}{2} \bar{\theta}_1^2 + \frac{\sigma_2}{2} \bar{\theta}_2^2 + \frac{\sigma_3}{2} \bar{\theta}_3^2$, $c \triangleq \frac{1}{\alpha_1} \min \left\{ k_e - \frac{1}{2} - \frac{1}{2} (\Delta_2 + \bar{\epsilon}_2), \sigma_1, \sigma_2 \right\}$, and σ_ℓ and Δ_ℓ are defined in Section IV-B.

The probability of $\|z(t)\| \leq \chi$ (i.e., $z(t) \in \mathcal{D}$) is equivalent to the probability that the Lyapunov function candidate remains below the threshold $m \triangleq \alpha_1 \chi^2$. Specifically, following (25), the condition $V_L(z) \leq m$ ensures that $\|z(t)\| \leq \chi$.

Lemma 1. For the Ito process $z \in \mathbb{R}^n$ and function V , assume

(A1) V is non-negative, $V(0) = 0$, and $V \in \mathcal{C}^2$ over the open and connected set $Q_m \triangleq \{z : V(z) < m\}$, where $m \in \mathbb{R}_{>0}$ is a bounding constant,

(A2) $z(t)$ is a continuous strong Markov process defined until at least some $\tau' > \tau_m = \inf \{t : z(t) \notin Q_m\}$ with probability one,²

If $\mathcal{L}V(z) \leq -\kappa_1 V(z) + \kappa_2$ in Q_m for $\kappa_1, \kappa_2 > 0$, then for $\lambda \leq m$, $z(t)$ is UUB-p with the probability

$$\mathbb{P} \left(\sup_{t \leq s < \infty} V(z(s)) \geq \lambda \right) \leq \frac{1}{m} V(z(0)) + \frac{1}{\lambda} V(z(0)) \exp(-\kappa_1 t) + \frac{\kappa_2}{\kappa_1 \lambda}.$$

²This assumption guarantees the existence of the process up to τ' with probability one, an essential requirement for the validity of the analysis.

Proof: See Appendix. ■

To facilitate the subsequent analysis, the following gain condition is introduced

$$k_e > \frac{1}{2} + \frac{1}{2} (\Delta_2 + \bar{\epsilon}_2). \quad (28)$$

Additionally, let the escape risk of z be defined as

$$\vartheta \triangleq \frac{1}{m} V_L(z(0)) + \frac{1}{\lambda} V_L(z(0)) e^{-ct} + \frac{b}{c\lambda}. \quad (29)$$

To ensure $\vartheta \in (0, 1)$ and the set \mathcal{S} defined in (26) is non-empty, the following feasibility condition is introduced

$$\chi \geq \sqrt{\frac{\alpha_2 b}{\alpha_1 c} \sqrt{\frac{\alpha_2}{\alpha_1} + 1}}. \quad (30)$$

Recall the set of stabilizing initial conditions in (26). In the subsequent analysis, it is shown that if $z(0) \in \mathcal{S} \subseteq \mathcal{D}$, then $z(t)$ is UUB-p and does not escape \mathcal{D} with a probability with the bound of $1 - \vartheta$. The following theorem states the main result of this paper.

Theorem 1. Consider the stochastic dynamical system in (10). Let (28) and (30) hold. For any initial conditions of the states $z(0) \in \mathcal{S}$, the update laws and controller given by (18)-(22) ensure that the solution $z(t)$ is UUB-p in the sense that

$$\mathbb{P} \left(\sup_{t \leq s < \infty} \|z(s)\| < \sqrt{\frac{\lambda}{\alpha_1}} \right) \geq 1 - \vartheta. \quad (31)$$

Proof: Taking the infinitesimal generator of the candidate Lyapunov function in (24) yields

$$\mathcal{L}V_L(z) = \frac{\partial V_L}{\partial z} F(z) + \frac{1}{2} \text{tr} \left(G(z, t)^\top \frac{\partial^2 V_L}{\partial z^2} G(z, t) \right). \quad (32)$$

Substituting $F(z)$, $G(z, t)$, and values of $\frac{\partial V_L}{\partial e}$ and $\frac{\partial^2 V_L}{\partial e^2}$ into (32), using the fact that $e^\top e$ is a scalar, applying the trace property in (3), and incorporating (17) and the fact that θ_ℓ^* is a constant for all $\ell \in \{1, 2, 3\}$ yields

$$\begin{aligned} \mathcal{L}V_L = & e^\top \left(f(x) - k_e e - \Phi_1(x, \hat{\theta}_1) - \frac{1}{2} e \Phi_2(x, \hat{\theta}_2) - \Phi_3(x, \hat{\theta}_3) \right) \\ & + \frac{1}{2} \text{tr} \left(g_2^\top g_2 \Sigma \Sigma^\top \right) - \bar{\theta}_1^\top \gamma_1^{-1} \text{proj} \left(\gamma_1 \Phi_1'^\top(x, \hat{\theta}_1) e - \gamma_1 \sigma_1 \hat{\theta}_1 \right) \\ & - \bar{\theta}_2^\top \gamma_2^{-1} \text{proj} \left(\frac{1}{2} \gamma_2 e^\top e \Phi_2'^\top(x, \hat{\theta}_2) - \gamma_2 \sigma_2 \hat{\theta}_2 \right) \\ & - \bar{\theta}_3^\top \gamma_3^{-1} \text{proj} \left(\gamma_3 \Phi_3'^\top(x, \hat{\theta}_3) e - \gamma_3 \sigma_3 \hat{\theta}_3 \right). \end{aligned} \quad (33)$$

Using the definition of the Frobenius norm on the term $\text{tr}(g_2^\top g_2 \Sigma \Sigma^\top)$ yields

$$\text{tr}(g_2^\top g_2 \Sigma \Sigma^\top) = \text{tr}(\Sigma^\top g_2^\top g_2 \Sigma) = \text{tr}((g_2 \Sigma)^\top (g_2 \Sigma)) = \|g_2 \Sigma(t)\|_F^2. \quad (34)$$

Applying the Cauchy-Schwarz inequality [45, Page 189] to (34) yields

$$\|g_2 \Sigma(t)\|_F^2 \leq \|g_2\|_F^2 \|\Sigma(t)\|_F^2 = \text{tr}(g_2^\top g_2) \|\Sigma(t)\|_F^2. \quad (35)$$

Using (4), (34), (35), and the fact that $\|\Sigma(t)\|_F^2 \leq \sup_{t \in \mathbb{R}_{\geq 0}} \|\Sigma(t)\|_F^2 \triangleq \|\Sigma\|_{F\infty}^2$, the term $\text{tr}(g_2^\top g_2 \Sigma \Sigma^\top)$ in (33) is upper bounded as

$$\text{tr}(g_2^\top g_2 \Sigma \Sigma^\top) \leq \text{tr}(g_2^\top g_2) \|\Sigma\|_{F\infty}^2. \quad (36)$$

Thus, applying (36) to (33), applying the trace-to-vector property in (2) to $\text{tr}(g_2^\top g_2)$, and substituting (12) into (33) yields

$$\begin{aligned} \mathcal{L}V_L &= e^\top \left(f(x) - k_e e - \Phi_1(x, \hat{\theta}_1) - \frac{1}{2} e \Phi_2(x, \hat{\theta}_2) - \Phi_3(x, \hat{\theta}_3) \right) \\ &\quad + \frac{1}{2} \|\Sigma\|_{F\infty}^2 \left(e^\top \Psi(x)^\top \Psi(x) e + 2e^\top \Psi(x)^\top \text{vec}(g_2(x_d)) \right. \\ &\quad \left. + \text{vec}(g_2(x_d))^\top \text{vec}(g_2(x_d)) \right) \\ &\quad - \bar{\theta}_1^\top \gamma_1^{-1} \text{proj} \left(\gamma_1 \Phi_1'^\top(x, \hat{\theta}_1) e - \gamma_1 \sigma_1 \hat{\theta}_1 \right) \\ &\quad - \bar{\theta}_2^\top \gamma_2^{-1} \text{proj} \left(\frac{1}{2} \gamma_2 e^\top e \Phi_2'^\top(x, \hat{\theta}_2) - \gamma_2 \sigma_2 \hat{\theta}_2 \right) \\ &\quad - \bar{\theta}_3^\top \gamma_3^{-1} \text{proj} \left(\gamma_3 \Phi_3'^\top(x, \hat{\theta}_3) e - \gamma_3 \sigma_3 \hat{\theta}_3 \right). \end{aligned} \quad (37)$$

Applying the Cauchy-Schwarz inequality to $\frac{1}{2} \|\Sigma\|_{F\infty}^2 e^\top \Psi^\top \Psi e$ yields

$$\begin{aligned} &\frac{1}{2} \|\Sigma\|_{F\infty}^2 e^\top \Psi^\top \Psi e = \frac{1}{2} \|\Sigma\|_{F\infty}^2 \|\Psi e\|^2 \\ &\leq \frac{1}{2} \|\Sigma\|_{F\infty}^2 \|\Psi\|_F^2 \|e\|^2 = \frac{1}{2} \|\Sigma\|_{F\infty}^2 e^\top \text{ctr} \left\{ \Psi(x)^\top \Psi(x) \right\}. \end{aligned} \quad (38)$$

Thus, applying (38) and (14)-(16) to (37), and upper-bounding $\text{vec}(g_2(x_d))$ as $\text{vec}(g_2(x_d)) \leq \|\text{vec}(g_2(x_d))\| \leq \bar{g}$, yields

$$\begin{aligned} \mathcal{L}V_L &= e^\top \left(\Phi_1(x, \theta_1) + \varepsilon_1(x) - k_e e - \Phi_1(x, \hat{\theta}_1) - \frac{1}{2} e \Phi_2(x, \hat{\theta}_2) \right. \\ &\quad \left. - \Phi_3(x, \hat{\theta}_3) \right) + \frac{1}{2} e^\top e (\Phi_2(x, \theta_2) + \varepsilon_2(x)) + e^\top (\Phi_3(x, \theta_3) + \varepsilon_3(x)) \\ &\quad + \frac{1}{2} \|\Sigma\|_{F\infty}^2 \bar{g}^2 - \bar{\theta}_1^\top \gamma_1^{-1} \text{proj} \left(\gamma_1 \Phi_1'^\top(x, \hat{\theta}_1) e - \gamma_1 \sigma_1 \hat{\theta}_1 \right) \\ &\quad - \bar{\theta}_2^\top \gamma_2^{-1} \text{proj} \left(\frac{1}{2} \gamma_2 e^\top e \Phi_2'^\top(x, \hat{\theta}_2) - \gamma_2 \sigma_2 \hat{\theta}_2 \right) \\ &\quad - \bar{\theta}_3^\top \gamma_3^{-1} \text{proj} \left(\gamma_3 \Phi_3'^\top(x, \hat{\theta}_3) e - \gamma_3 \sigma_3 \hat{\theta}_3 \right). \end{aligned} \quad (39)$$

From [43, P2 in Thm. 1], $\gamma_3 \Phi_3'^\top(x, \hat{\theta}_3) e - \gamma_3 \sigma_3 \hat{\theta}_3 \leq \text{proj}(\gamma_3 \Phi_3'^\top(x, \hat{\theta}_3) e - \gamma_3 \sigma_3 \hat{\theta}_3)$. Applying this inequality to (39), substituting (21) into (39), and cancelling the cross terms, incorporating (17), and utilizing the bounds on the reconstruction errors and the higher order terms yields

$$\begin{aligned} \mathcal{L}V_L &\leq -k_e e^\top e - \sigma_1 \bar{\theta}_1^\top \bar{\theta}_1 - \sigma_2 \bar{\theta}_2^\top \bar{\theta}_2 - \sigma_3 \bar{\theta}_3^\top \bar{\theta}_3 \\ &\quad + |e^\top| (\Delta_1 + \bar{\varepsilon}_1) + \frac{1}{2} e^\top e (\Delta_2 + \bar{\varepsilon}_2) + |e^\top| (\Delta_3 + \bar{\varepsilon}_3) \\ &\quad + \frac{1}{2} \|\Sigma\|_{F\infty}^2 \bar{g}^2 + \sigma_1 \bar{\theta}_1^\top \theta_1^* + \sigma_2 \bar{\theta}_2^\top \theta_2^* + \sigma_3 \bar{\theta}_3^\top \theta_3^*, \end{aligned} \quad (40)$$

when $z \in \mathcal{D}$. Applying Young's inequality on the terms $|e^\top| (\Delta_1 + \bar{\varepsilon}_1 + \Delta_3 + \bar{\varepsilon}_3)$, $\sigma_\ell \bar{\theta}_\ell^\top \theta_\ell^*$, for all $\ell \in \{1, 2, 3\}$, incorporating z and the gain condition $k_e > \frac{1}{2} + \frac{1}{2} (\Delta_2 + \bar{\varepsilon}_2)$ leads to

$$\mathcal{L}V_L \leq -c_1 \|z\|^2 + b,$$

when $z \in \mathcal{D}$. Using the upper-bound $V_L \leq \alpha_2 \|z\|^2$ introduced in (25) yields

$$\mathcal{L}V_L \leq -cV_L + b, \quad (41)$$

when $z \in \mathcal{D}$. Since $V_L(0) = 0$, $V_L \in \mathcal{C}^2$, and z is a continuous strong Markov process, then assumptions (A1) and (A2) in Lemma 1 is satisfied. Therefore, from (41) and Lemma

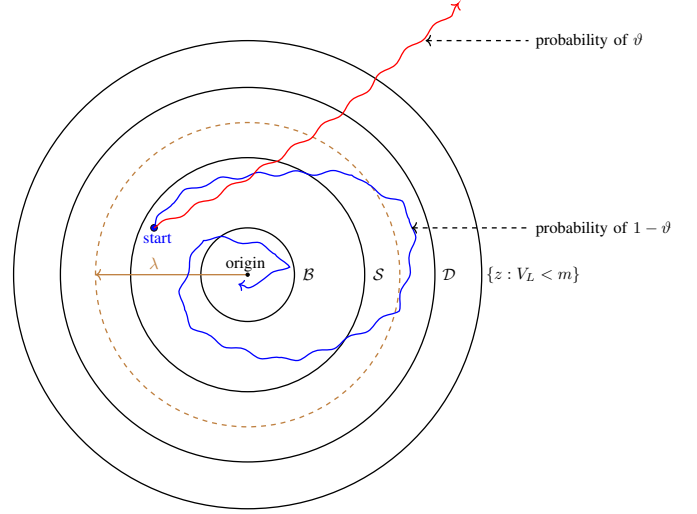


Figure 1. For a UUB-p system, if the states are initialized within the set \mathcal{S} , they remain inside the set \mathcal{D} with probability $1 - \vartheta$ and eventually exponentially converge to the set \mathcal{D} , staying within the bounded set (blue trajectory). However, there is an escape risk of ϑ , meaning the trajectories can potentially be unbounded (red trajectory). Additionally, λ is the radius of an arbitrary level set, whose size corresponds to either the minimum size of \mathcal{B} or the maximum size of $\{z : V_L < m\}$.

1, $\mathbb{P} \left(\sup_{t \leq s < \infty} V_L(z(s)) \geq \lambda \right) \leq \vartheta$, when $z \in \mathcal{D}$, which is equivalent to

$$\mathbb{P} \left(\sup_{t \leq s < \infty} V_L(z(s)) < \lambda \right) \geq 1 - \vartheta. \quad (42)$$

From (25), $\mathbb{P} \left(\sup_{t \leq s < \infty} \|z(s)\|^2 < \frac{\lambda}{\alpha_1} \right) \geq \mathbb{P} \left(\sup_{t \leq s < \infty} V_L(z(s)) < \lambda \right)$. Therefore, using (42) and Lemma 1 yields (31), when $z(t) \in \mathcal{D}$. From (31) and Definition 1, the solution $z(t)$ is UUB-p with $z \in \mathcal{D}$.

To establish the universal approximation property, it suffices to show that $\mathbf{x} \in \Omega_2$, where Ω_2 was introduced in (13). By construction, $x_d \in \Omega_1$. Now, let $\iota \in \mathbb{R}^\varphi$. Since $z \in \mathcal{D}$, $x \in \Omega_1$. Furthermore, since $z \in \mathcal{D}$, $e \in \mathcal{D}$ which implies $\|x - x_d\| \leq \chi$. Using triangle inequality, $\|x\| - \|x_d\| \leq \chi$ which implies $\|x\| \leq \chi + \bar{x}_d$. Therefore, $x \in \Omega_1$. Since $\{\mathbf{x} : x, x_d \in \Omega_1\} \subset \{\mathbf{x} : \mathbf{x} \in \Omega_2\}$, it is concluded that $\mathbf{x} \in \Omega_2$.

The analysis so far involves the condition $z(t) \in \mathcal{D}$ (see, Figure 1). To obtain conditions with probability bounds for when $z(t) \in \mathcal{D}$, let $S_1 \triangleq \{z : \|z(t)\| < \sqrt{\frac{\lambda}{\alpha_1}}\}$ and $S_2 \triangleq \{z : \|z(t)\| < \sqrt{\frac{m}{\alpha_1}}\}$. Since $S_1 \subseteq S_2$, by substituting $m = \alpha_1 \chi^2$ into S_2 and invoking the monotonicity property in (6), $\mathbb{P} \left(\sup_{t \leq s < \infty} \|z(s)\| < \chi \right) \geq \mathbb{P} \left(\sup_{t \leq s < \infty} \|z(s)\| < \sqrt{\frac{\lambda}{\alpha_1}} \right)$. Therefore, this inequality together with (31) yields $\mathbb{P} \left(\sup_{t \leq s < \infty} \|z(s)\| < \chi \right) \geq 1 - \vartheta$ which ensures $z(t) \in \mathcal{D}$ with the probability of $1 - \vartheta$.

To ensure the states remain bounded, it needs to be shown that $\mathcal{S} \subseteq \mathcal{D}$. Consider any $\iota_1 \in \mathbb{R}^\varphi$ and let $\iota_1 \in \mathcal{S}$. From (26), $\|\iota_1\| \leq \sqrt{\frac{1}{\alpha_2} \sqrt{\frac{\alpha_1}{\alpha_2} \chi^2 - \frac{b}{c}}} \leq \sqrt{\frac{1}{\alpha_2} \sqrt{\frac{\alpha_1}{\alpha_2} \chi}} \leq \chi$. Since $\alpha_2 > 1$ and $\alpha_1 < \alpha_2$, $\|\iota_1\| \leq \sqrt{\frac{1}{\alpha_2} \sqrt{\frac{\alpha_1}{\alpha_2} \chi}} \leq \chi$, implying that $\iota_1 \in \mathcal{D}$. Therefore, $\mathcal{S} \subseteq \mathcal{D}$.

To ensure the states converge to a subset of the set of stabilizing initial conditions, it suffices to show $\mathcal{B} \subseteq \mathcal{S}$. Consider any $\iota_2 \in \mathbb{R}^\varphi$ and let $\iota_2 \in \mathcal{B}$. Solving the condition $\chi \geq \sqrt{\frac{\alpha_2 b}{\alpha_1 c} \sqrt{\frac{\alpha_2}{\alpha_1} + 1}}$ for $\sqrt{\frac{b}{c\alpha_1}}$ yields $\sqrt{\frac{b}{c\alpha_1}} \leq \sqrt{\frac{1}{\alpha_2} \sqrt{\frac{\alpha_1}{\alpha_2} \chi^2 - \frac{b}{c}}}$, where the obtained inequality together with the definition of \mathcal{B} in (27) yields $\|\iota_2\| \leq \sqrt{\frac{b}{c\alpha_1}} \leq \sqrt{\frac{1}{\alpha_2} \sqrt{\frac{\alpha_1}{\alpha_2} \chi^2 - \frac{b}{c}}}$, implying that $\iota_2 \in \mathcal{S}$. Therefore, $\mathcal{B} \subseteq \mathcal{S}$. Finally, since $\chi \leq \chi + 2\bar{x}_d$, from the definitions of sets \mathcal{D} and Ω_2 , it is ensured that $\mathcal{D} \subseteq \{z : \mathbf{x} \in \Omega_2\}$. Therefore, $\mathcal{B} \subseteq \mathcal{S} \subseteq \mathcal{D} \subseteq \{z : \mathbf{x} \in \Omega_2\}$.

Recall $S_1 \triangleq \{z : \|z\| < \sqrt{\frac{\lambda}{\alpha_1}}\}$, and let $S_3 \triangleq \{z : \|e\| < \sqrt{\frac{\lambda}{\alpha_1}}\}$. Since $S_1 \subseteq S_3$, the monotonicity property in (6) yields $\mathbb{P}\left(\sup_{t \leq s < \infty} \|z(s)\| < \sqrt{\frac{\lambda}{\alpha_1}}\right) \leq \mathbb{P}\left(\sup_{t \leq s < \infty} \|e(s)\| < \sqrt{\frac{\lambda}{\alpha_1}}\right)$. This inequality together with (31) yields $\mathbb{P}\left(\sup_{t \leq s < \infty} \|e(s)\| < \sqrt{\frac{\lambda}{\alpha_1}}\right) \geq 1 - \vartheta$. Let $S_4 \triangleq \{z : \|x\| < \sqrt{\frac{\lambda}{\alpha_1} + \bar{x}_d}\}$. Since $S_3 \subseteq S_4$, the monotonicity property in (6) yields $\mathbb{P}\left(\sup_{t \leq s < \infty} \|x(s)\| < \sqrt{\frac{\lambda}{\alpha_1} + \bar{x}_d}\right) \geq \mathbb{P}\left(\sup_{t \leq s < \infty} \|e(s)\| < \sqrt{\frac{\lambda}{\alpha_1}}\right) \geq 1 - \vartheta$. Let $S_{5,\ell} \triangleq \{z : \|\hat{\theta}_\ell\| < \sqrt{\frac{\lambda}{\alpha_1}}\}$, for all $\ell \in \{1, 2, 3\}$. Since $S_1 \subseteq S_{5,\ell}$, the monotonicity property yields $\mathbb{P}\left(\sup_{t \leq s < \infty} \|\hat{\theta}_\ell(s)\| < \sqrt{\frac{\lambda}{\alpha_1}}\right) \geq \mathbb{P}\left(\sup_{t \leq s < \infty} \|z(s)\| < \sqrt{\frac{\lambda}{\alpha_1}}\right)$, for all $\ell \in \{1, 2, 3\}$. This obtained inequality together with (31) yields $\mathbb{P}\left(\sup_{t \leq s < \infty} \|\hat{\theta}_\ell(s)\| < \sqrt{\frac{\lambda}{\alpha_1}}\right) \geq 1 - \vartheta$, for all $\ell \in \{1, 2, 3\}$. Since $\mathbb{P}\left\{\sup_{t \leq s < \infty} \|x(s)\| < \sqrt{\frac{\lambda}{\alpha_1} + \bar{x}_d}\right\} \geq 1 - \vartheta$ and $\hat{\theta}_\ell$ is bounded, and based on the smoothness of $\Phi_1(x, \hat{\theta}_1)$, $\Phi_2(x, \hat{\theta}_2)$, and $\Phi_3(\mathbf{x}, \hat{\theta}_3)$ there exists a constant $\bar{\Phi}_\ell \in \mathbb{R}_{>0}$ such that $\mathbb{P}\left(\sup_{t \leq s < \infty} \|\Phi_1(x(s), \hat{\theta}_1(s))\| \leq \bar{\Phi}_1\right) \geq 1 - \vartheta$, $\mathbb{P}\left(\sup_{t \leq s < \infty} \|\Phi_2(x(s), \hat{\theta}_2(s))\| \leq \bar{\Phi}_2\right) \geq 1 - \vartheta$, and $\mathbb{P}\left(\sup_{t \leq s < \infty} \|\Phi_3(\mathbf{x}(s), \hat{\theta}_3(s))\| \leq \bar{\Phi}_3\right) \geq 1 - \vartheta$, for all $\ell \in \{1, 2, 3\}$. Since $\mathbb{P}\left(\sup_{t \leq s < \infty} \|\Phi(x(s), \hat{\theta}_1(s))\| \leq \bar{\Phi}_1\right) \geq 1 - \vartheta$, $\mathbb{P}\left(\sup_{t \leq s < \infty} \|\Phi(x(s), \hat{\theta}_2(s))\| \leq \bar{\Phi}_2\right) \geq 1 - \vartheta$, $\mathbb{P}\left(\sup_{t \leq s < \infty} \|\Phi(\mathbf{x}(s), \hat{\theta}_3(s))\| \leq \bar{\Phi}_3\right) \geq 1 - \vartheta$, and

$\mathbb{P}\left(\sup_{t \leq s < \infty} \|e(s)\| < \sqrt{\frac{\lambda}{\alpha_1}}\right) \geq 1 - \vartheta$, using Assumption 2 and (22) yields $\mathbb{P}\left(\sup_{t \leq s < \infty} \|u(s)\| \leq \bar{u}\right) \geq 1 - \vartheta$, for some constant $\bar{u} \in \mathbb{R}_{>0}$. Therefore, all implemented signals are bounded with probability of $1 - \vartheta$. ■

VI. SIMULATION

To determine the efficacy of the proposed Lb-DNN adaptive controller, two simulations are performed on a five-dimensional nonlinear stochastic dynamical system, where f , g_2 , and Σ in (10) are defined as

$$f = \begin{bmatrix} x_4 \sqrt{|x_3|} + \sin(x_1) + x_5^2 x_2 \\ 1.5x_3^2 x_5 + \cos(x_3 + x_4) + x_1 \sqrt{|x_2|} \sin(x_3) \\ x_5^2 - x_3^3 x_4^2 \\ (x_1 x_3 - x_2)^3 \\ -x_1 x_5 \end{bmatrix},$$

$$g_2 = \begin{bmatrix} x_1 \cos(x_2) & 1 - x_3 \cos(x_4) \\ x_3 x_5 & x_4^2 \sin^2(x_2) \\ x_1^2 & x_3 \cos(x_1 x_2) \\ (x_1 + x_2)^3 - \sin(x_3) & 1 - x_3^2 \\ x_2 \sin^2(x_3) & -x_5 + x_1 x_4^2 \end{bmatrix},$$

$$\Sigma = \begin{bmatrix} \sin^2(t) & 0 \\ 0 & \exp(-t) \end{bmatrix},$$

where $x \triangleq [x_1, x_2, x_3, x_4, x_5]^\top : \mathbb{R}_{\geq 0} \rightarrow \mathbb{R}^3$ denotes the system state, and $g_1 = I_{5 \times 5}$. The simulations are performed for 60 seconds with initial condition $x(0) = [2, -1, 2, -1, 2]^\top$. The desired trajectory is selected as

$$x_d = \begin{bmatrix} \sin(2t) \\ -\cos(t) \\ \sin(3t) + \cos(-2t) \\ \sin(t) - \cos(-0.5t) \\ \sin(-t) \end{bmatrix}.$$

Two simulations are performed; the first one represents the performance of the developed Lb-DNN controller, and the second one illustrates the tracking performance of the controller in response to variations in mean and covariance of the stochastic noise. For the first simulation, the Wiener process, ω , is generated with mean of 0 and covariance of 1, whereas for the second simulation, the noise mean varies from -0.1 to 0.1 and the noise covariance ranges from 1 to 10. For both of the simulations, the learning rates and forgetting factors for each of the Lb-DNNs are selected as $\gamma_1 = \gamma_3 = 25$, $\gamma_2 = 5$, $\sigma_1 = \sigma_3 = 0.01$, and $\sigma_2 = 0.1$, respectively. For both simulations, the control gain in (22) is selected as $k_e = 500$. Both Lb-DNNs have $k_1 = k_2 = k_3 = 8$ inner layers with $L_1 = L_2 = L_3 = 8$ neurons per hidden layer. In these simulations, the Lb-DNNs use swish activation functions (see [46]). Since swish activation, a smooth approximation of ReLU activation, is used for the simulations, the weight estimates are initialized via Kaiming He initialization (see [47]).

Based on Figure 2, the tracking error demonstrates an exponential convergence to its ultimate bound. The developed Lb-DNN controller achieves a root-mean-square (RMS) tracking error norm of 0.533. Figure 3 illustrates the evolution of the

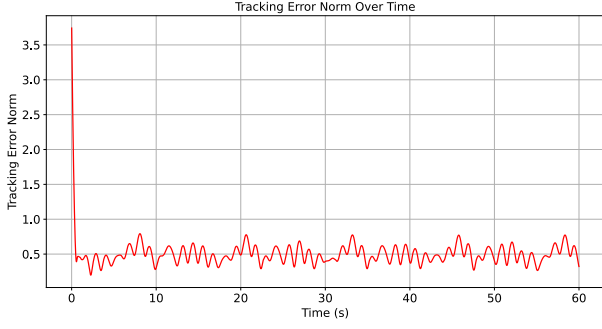


Figure 2. Performance of the tracking error over time for the developed Lb-DNN controller.

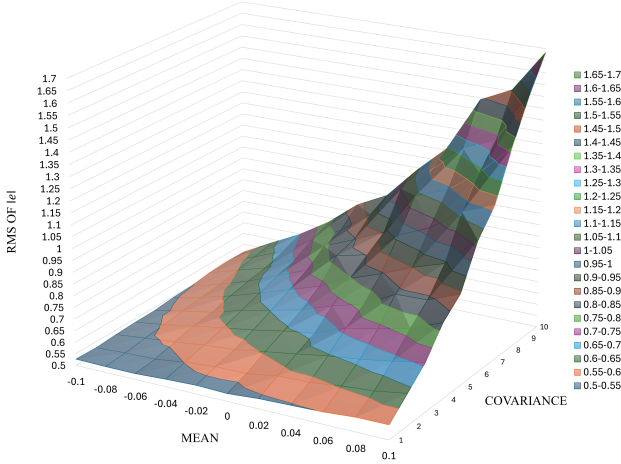


Figure 3. Performance of the RMS of the tracking error with respect to changes in mean and covariance of the stochastic noise for the developed Lb-DNN controller.

RMS of the norm of the tracking error in response to variations in the mean and covariance of the stochastic noise. As shown in Figure 3, the RMS tracking error tends to increase as noise mean and covariance grow. The smallest RMS tracking error of 0.524 occurs at a noise mean of -0.1 and a covariance of 2, whereas the largest RMS tracking error of 1.684 is observed at a noise mean of 0.1 and a covariance of 10.

VII. CONCLUSION

An Lb-DNN adaptive controller is developed for a stochastic process modeled by a control-affine nonlinear stochastic differential equation to achieve a trajectory tracking objective. Three Lb-DNNs are developed to compensate for deterministic and non-deterministic uncertainties within the closed-loop error system. The proposed Lb-DNN adaptive controller and the stability-driven update laws ensure the tracking error is uniformly ultimately bounded in probability, with a rigorous probability analysis. The result is supported by a probability analysis without the common assumption of vanishing noise and in the presence of unstructured model uncertainty. Simulations are performed on a nonlinear stochastic dynamical system to show the efficacy of the proposed method.

APPENDIX

Proof of Lemma 1

Let the strong Markov process $\tilde{z}(t)$ be defined as

$$\tilde{z}(t) \triangleq \begin{cases} z(t), & \text{for } t < \tau_m, \\ 0, & \text{for } t \geq \tau_m. \end{cases} \quad (43)$$

Notice that if $t \geq \tau_m$, then $\|\tilde{z}(t)\| = 0$, and if $t < \tau_m$, then $\|\tilde{z}(t)\| = \|z(t)\|$. Therefore, since V is non-negative and $V(0) = 0$ (according to (A1)), $V(\tilde{z}(t)) \leq V(z(t))$. Hence, the following relation holds for all $t \in \mathbb{R}_{\geq 0}$

$$\mathbb{E}[V(\tilde{z}(t))] \leq \mathbb{E}[V(z(t))]. \quad (44)$$

The solution to stochastic differential inequality given by $\mathcal{L}V(z) \leq -\kappa_1 V(z) + \kappa_2$ is (see [2, Thm. 4.1])

$$\mathbb{E}[V(z)] \leq V(z(0)) \exp(-\kappa_1 t) + \frac{\kappa_2}{\kappa_1}, \quad (45)$$

for all $t \in \mathbb{R}_{\geq 0}$. Applying (45) on (44) yields

$$\mathbb{E}[V(\tilde{z})] \leq V(z(0)) \exp(-\kappa_1 t) + \frac{\kappa_2}{\kappa_1}, \quad (46)$$

for all $t \in \mathbb{R}_{\geq 0}$.

The solution of $\mathcal{L}V$ given in (45) shows that $\mathbb{E}[V(z)]$ strictly decreases until it reaches the bound $\frac{\kappa_2}{\kappa_1}$. Once $\mathbb{E}[V(z)]$ reaches this bound, it stays bounded by $\frac{\kappa_2}{\kappa_1}$. However, inside this bound, $\mathbb{E}[V(z)]$ may increase, decrease, or stay constant. With this explanation provided, different cases of behavior of $\mathbb{E}[V(z)]$ are investigated here. To study the behavior of $\mathbb{E}[V(z)]$ before reaching the ultimate bound, let $\tau_B \triangleq \inf \{t \geq 0 : V(\tilde{z}(t)) \leq \frac{\kappa_2}{\kappa_1}\}$. For $t \in [0, \tau_B)$, V is a supermartingale (see [48, Thm. C.4]). Applying Doob's maximal inequality (see [49, Page 275]) and (46) yields

$$\begin{aligned} \mathbb{P} \left(\sup_{0 \leq t \leq s < \tau_B} V(\tilde{z}(s)) \geq \lambda \right) &\leq \frac{1}{\lambda} \mathbb{E} \left[\lim_{t \rightarrow \tau_B^-} V(\tilde{z}(t)) \right] \\ &\leq \frac{1}{\lambda} \mathbb{E}[V(\tilde{z}(t))] \leq \frac{1}{\lambda} \left(V(z(0)) \exp(-\kappa_1 t) + \frac{\kappa_2}{\kappa_1} \right). \end{aligned} \quad (47)$$

To study the behavior of $\mathbb{E}[V(z)]$ after reaching the ultimate bound, consider the interval $\mathcal{I} = [\tau_B, \infty)$. Without loss of generality, partition this interval into subintervals, defining $\mathcal{I} = [\tau_B, \tau_1) \cup [\tau_1, \tau_2) \cup [\tau_2, \tau_3) \cup [\tau_3, \infty)$, where each subinterval corresponds to a specific behavior of the process V : on $[\tau_B, \tau_1)$, V is a supermartingale; on $[\tau_1, \tau_2)$, a submartingale; and on $[\tau_2, \tau_3)$, a martingale.

For $t \in [\tau_B, \tau_1)$, since V is a supermartingale, using Doob's maximal inequality and (46) yields

$$\begin{aligned} \mathbb{P} \left(\sup_{\tau_B \leq t \leq s < \tau_1} V(\tilde{z}(s)) \geq \lambda \right) &\leq \frac{1}{\lambda} \mathbb{E} \left[\lim_{t \rightarrow \tau_1^-} V(\tilde{z}(t)) \right] \\ &\leq \frac{1}{\lambda} \mathbb{E}[V(\tilde{z}(t))] \leq \frac{1}{\lambda} \left(V(z(0)) \exp(-\kappa_1 t) + \frac{\kappa_2}{\kappa_1} \right). \end{aligned} \quad (48)$$

For $t \in [\tau_1, \tau_2)$, since V is a submartingale (see [48, Thm. C.4]), using Doob's maximal inequality yields

$$\begin{aligned} \mathbb{P} \left(\sup_{\tau_1 \leq t \leq s < \tau_2} V(\tilde{z}(s)) \geq \lambda \right) &\leq \frac{1}{\lambda} \mathbb{E} \left[\lim_{t \rightarrow \tau_2^-} V(\tilde{z}(t)) \right] \\ &\leq \frac{1}{\lambda} \frac{\kappa_2}{\kappa_1} \leq \frac{1}{\lambda} \left(V(z(0)) \exp(-\kappa_1 t) + \frac{\kappa_2}{\kappa_1} \right). \end{aligned} \quad (49)$$

For $t \in [\tau_2, \tau_3)$, since V is a martingale, using Doob's maximal inequality and (46) yields

$$\begin{aligned} & \mathbb{P} \left(\sup_{\tau_2 \leq t \leq s < \tau_3} V(\tilde{z}(s)) \geq \lambda \right) \leq \frac{1}{\lambda} \mathbb{E} \left[\lim_{t \rightarrow \tau_3^-} V(\tilde{z}(t)) \right] \\ & \leq \frac{1}{\lambda} \mathbb{E} [V(\tilde{z}(t))] \leq \frac{1}{\lambda} \left(V(z(0)) \exp(-\kappa_1 t) + \frac{\kappa_2}{\kappa_1} \right). \end{aligned} \quad (50)$$

Since $[0, \infty) = [0, \tau_B) \cup \mathcal{I}$, and the bounds over each time interval are identical, no generality is lost. Therefore, using (47)-(50) yields

$$\mathbb{P} \left(\sup_{t \leq s < \infty} V(\tilde{z}(s)) \geq \lambda \right) \leq \frac{1}{\lambda} \left(V(z(0)) \exp(-\kappa_1 t) + \frac{\kappa_2}{\kappa_1} \right). \quad (51)$$

Note that for $t \geq \tau_m$, $V(\tilde{z}(t)) \neq V(z(t))$. Then, it holds that

$$\begin{aligned} & \mathbb{P} \left(\sup_{t \leq s < \infty} |V(\tilde{z}(s)) - V(z(s))| \geq \lambda \right) \\ & \leq \mathbb{P} \left(\sup_{0 \leq s < \infty} |V(\tilde{z}(s)) - V(z(s))| \geq \lambda \right). \end{aligned} \quad (52)$$

For $t \leq \tau_m$, where $V(\tilde{z}(t)) = V(z(t))$, it follows that $\mathbb{P} \left(\sup_{t \leq s < \infty} V(\tilde{z}(s)) \geq \lambda \right) = \mathbb{P} \left(\sup_{t \leq s < \infty} V(z(s)) \geq \lambda \right)$. Therefore,

$$\begin{aligned} & \left| \mathbb{P} \left(\sup_{t \leq s < \infty} V(\tilde{z}(s)) \geq \lambda \right) - \mathbb{P} \left(\sup_{t \leq s < \infty} V(z(s)) \geq \lambda \right) \right| \\ & = \mathbb{P} \left(\sup_{t \leq s < \infty} |V(\tilde{z}(s)) - V(z(s))| \geq \lambda \right) = 0. \end{aligned} \quad (53)$$

Similarly, when $t > \tau_m$, $V(\tilde{z}(t)) = 0$, which implies $\mathbb{P} \left(\sup_{t \leq s < \infty} V(\tilde{z}(s)) \geq \lambda \right) = 0$, ensuring that (53) holds for all $t \in \mathbb{R}_{>0}$. Applying the triangle inequality on the left side of (53) yields

$$\begin{aligned} & \left| \mathbb{P} \left(\sup_{t \leq s < \infty} V(z(s)) \geq \lambda \right) - \mathbb{P} \left(\sup_{t \leq s < \infty} V(\tilde{z}(s)) \geq \lambda \right) \right| \\ & \leq \left| \mathbb{P} \left(\sup_{t \leq s < \infty} V(\tilde{z}(s)) \geq \lambda \right) - \mathbb{P} \left(\sup_{t \leq s < \infty} V(z(s)) \geq \lambda \right) \right|. \end{aligned} \quad (54)$$

Solving for $\mathbb{P} \left(\sup_{t \leq s < \infty} V(z(s)) \geq \lambda \right)$ in (54), and using (52) and (53) yields

$$\begin{aligned} \mathbb{P} \left(\sup_{t \leq s < \infty} V(z(s)) \geq \lambda \right) & \leq \mathbb{P} \left(\sup_{0 \leq s < \infty} |V(\tilde{z}(s)) - V(z(s))| \geq \lambda \right) \\ & + \mathbb{P} \left(\sup_{t \leq s < \infty} V(\tilde{z}(s)) \geq \lambda \right). \end{aligned} \quad (55)$$

Using Markov's inequality (see [49, Page 153]), it can be stated that

$$\begin{aligned} & \mathbb{P} \left(\sup_{0 \leq s < \infty} |V(\tilde{z}(s)) - V(z(s))| \geq \lambda \right) \\ & = \mathbb{P} \left(\sup_{0 \leq s < \infty} V(z(s)) \geq m \right) \leq \frac{1}{m} V(z(0)). \end{aligned} \quad (56)$$

Therefore, using (51), (55), and (56) yields

$$\begin{aligned} \mathbb{P} \left(\sup_{t \leq s < \infty} V(z(s)) \geq \lambda \right) & \leq \frac{1}{m} V(z(0)) \\ & + \frac{1}{\lambda} V(z(0)) \exp(-\kappa_1 t) + \frac{\kappa_2}{\kappa_1 \lambda}. \end{aligned} \quad (57)$$

REFERENCES

- [1] H. Deng and M. Krstić, "Stochastic nonlinear stabilization – I: A backstepping design," *Syst. & Control Lett.*, vol. 32, no. 3, pp. 143–150, 1997.
- [2] H. Deng, M. Krstic, and R. J. Williams, "Stabilization of stochastic nonlinear systems driven by noise of unknown covariance," *IEEE Trans. Autom. Control*, vol. 46, no. 8, pp. 1237–1253, 2001.
- [3] B. Jiang, H. R. Karimi, S. Yang, C. Gao, and Y. Kao, "Observer-based adaptive sliding mode control for nonlinear stochastic Markov jump systems via its fuzzy modeling: Applications to robot arm model," *IEEE Trans. Ind. Electron.*, vol. 68, no. 1, pp. 466–477, 2020.
- [4] V. Stojanovic and N. Nedic, "Joint state and parameter robust estimation of stochastic nonlinear systems," *Int. J. Robust & Nonlinear Control*, vol. 26, no. 14, pp. 3058–3074, 2016.
- [5] S.-J. Liu, J.-F. Zhang, and Z.-P. Jiang, "Decentralized adaptive output-feedback stabilization for large-scale stochastic nonlinear systems," *Automatica*, vol. 43, no. 2, pp. 238–251, 2007.
- [6] W. Li and M. Krstic, "Prescribed-time output-feedback control of stochastic nonlinear systems," *IEEE Trans. Autom. Control*, vol. 68, no. 3, pp. 1431–1446, 2022.
- [7] P. R. Kumar and P. Varaiya, *Stochastic systems: Estimation, identification, and adaptive control*. SIAM, 2015.
- [8] Q. Zhou, P. Shi, S. Xu, and H. Li, "Observer-based adaptive neural network control for nonlinear stochastic systems with time delay," *IEEE Trans. Neural Netw. & Learning Syst.*, vol. 24, no. 1, pp. 71–80, 2012.
- [9] W. Li and M. Krstic, "Stochastic adaptive nonlinear control with filterless least squares," *IEEE Trans. Autom. Control*, vol. 66, no. 9, pp. 3893–3905, 2020.
- [10] P. Shi, Y. Xia, G. Liu, and D. Rees, "On designing of sliding-mode control for stochastic jump systems," *IEEE Trans. Autom. Control*, vol. 51, no. 1, pp. 97–103, 2006.
- [11] W. Qi, G. Zong, and H. R. Karimi, "Sliding mode control for nonlinear stochastic singular semi-Markov jump systems," *IEEE Trans. Autom. Control*, vol. 65, no. 1, pp. 361–368, 2019.
- [12] C. P. Chen, Y.-J. Liu, and G.-X. Wen, "Fuzzy neural network-based adaptive control for a class of uncertain nonlinear stochastic systems," *IEEE Trans. Cybern.*, vol. 44, no. 5, pp. 583–593, 2013.
- [13] Y. Li, S. Sui, and S. Tong, "Adaptive fuzzy control design for stochastic nonlinear switched systems with arbitrary switchings and unmodeled dynamics," *IEEE Trans. Cybern.*, vol. 47, no. 2, pp. 403–414, 2016.
- [14] Y. Sun, B. Chen, C. Lin, H. Wang, and S. Zhou, "Adaptive neural control for a class of stochastic nonlinear systems by backstepping approach," *Inf. Sci.*, vol. 369, pp. 748–764, 2016.
- [15] J. Li, W. Chen, J. Li, and Y. Fang, "Adaptive NN output-feedback stabilization for a class of stochastic nonlinear strict-feedback systems," *ISA Trans.*, vol. 48, no. 4, pp. 468–475, 2009.
- [16] Z. Li, T. Li, G. Feng, R. Zhao, and Q. Shan, "Neural network-based adaptive control for pure-feedback stochastic nonlinear systems with time-varying delays and dead-zone input," *IEEE Trans. Syst., Man, & Cybern.: Syst.*, vol. 50, no. 12, pp. 5317–5329, 2018.
- [17] H. Wang, P. X. Liu, J. Bao, X.-J. Xie, and S. Li, "Adaptive neural output-feedback decentralized control for large-scale nonlinear systems with stochastic disturbances," *IEEE Trans. Neural Netw. & Learning Syst.*, vol. 31, no. 3, pp. 972–983, 2019.
- [18] L. Wang and C. P. Chen, "Reduced-order observer-based dynamic event-triggered adaptive NN control for stochastic nonlinear systems subject to unknown input saturation," *IEEE Trans. Neural Netw. & Learning Syst.*, vol. 32, no. 4, pp. 1678–1690, 2020.
- [19] F. Wang, Z. You, Z. Liu, and C. P. Chen, "A fast finite-time neural network control of stochastic nonlinear systems," *IEEE Trans. Neural Netw. & Learning Syst.*, vol. 34, no. 10, pp. 7443–7452, 2022.
- [20] W. Chen, L. Jiao, J. Li, and R. Li, "Adaptive NN backstepping output-feedback control for stochastic nonlinear strict-feedback systems with time-varying delays," *IEEE Trans. Syst., Man, & Cybern., Part B (Cybernetics)*, vol. 40, no. 3, pp. 939–950, 2009.
- [21] H. J. Kushner, *Introduction to Stochastic Control*. New York: Holt, Reinhart and Winston, 1971.
- [22] H. K. Khalil, *Nonlinear Systems*. Prentice Hall, 3 ed., 2002.
- [23] D. Rolnick and M. Tegmark, "The power of deeper networks for expressing natural functions," in *Int. Conf. Learn. Represent.*, 2018.
- [24] S. Liang and R. Srikant, "Why deep neural networks for function approximation?," *arXiv preprint arXiv:1610.04161*, 2016.
- [25] Z. Lamb, Z. I. Bell, M. Longmire, J. Paquet, P. Ganesh, and R. Sanfelice, "Deep nonlinear adaptive control for unmanned aerial systems operating under dynamic uncertainties," *arXiv preprint arXiv:2310.09502*, 2023.

- [26] S. L. Brunton and J. N. Kutz, *Data-driven science and engineering: Machine learning, dynamical systems, and control*. Cambridge University Press, 2019.
- [27] K. Noda, H. Arie, Y. Suga, and T. Ogata, "Multimodal integration learning of robot behavior using deep neural networks," *Robotics & Auton. Syst.*, vol. 62, no. 6, pp. 721–736, 2014.
- [28] D. Sarikaya, J. J. Corso, and K. A. Guru, "Detection and localization of robotic tools in robot-assisted surgery videos using deep neural networks for region proposal and detection," *IEEE Trans. Med. Imaging*, vol. 36, no. 7, pp. 1542–1549, 2017.
- [29] H.-T. Nguyen and C. C. Cheah, "Analytic deep neural network-based robot control," *IEEE/ASME Trans. Mechatron.*, vol. 27, no. 4, pp. 2176–2184, 2022.
- [30] O. Patil, D. Le, M. Greene, and W. E. Dixon, "Lyapunov-derived control and adaptive update laws for inner and outer layer weights of a deep neural network," *IEEE Control Syst Lett.*, vol. 6, pp. 1855–1860, 2022.
- [31] O. S. Patil, D. M. Le, E. Griffis, and W. E. Dixon, "Deep residual neural network (ResNet)-based adaptive control: A Lyapunov-based approach," in *Proc. IEEE Conf. Decis. Control*, pp. 3487–3492, 2022.
- [32] R. Hart, O. Patil, E. Griffis, and W. E. Dixon, "Deep Lyapunov-based physics-informed neural networks (DeLb-PINN) for adaptive control design," in *Proc. IEEE Conf. Decis. Control*, pp. 1511–1516, 2023.
- [33] C. F. Nino, O. S. Patil, J. Philor, Z. Bell, and W. E. Dixon, "Deep adaptive indirect herding of multiple target agents with unknown interaction dynamics," in *Proc. IEEE Conf. Decis. Control*, pp. 2509–2514, 2023.
- [34] E. Griffis, O. Patil, W. Makumi, and W. E. Dixon, "Deep recurrent neural network-based observer for uncertain nonlinear systems," in *IFAC World Congr.*, pp. 6851–6856, 2023.
- [35] J. Chen, J. Mei, J. Hu, and Z. Yang, "Deep neural networks-prescribed performance optimal control for stochastic nonlinear strict-feedback systems," *Neurocomp.*, p. 128633, 2024.
- [36] J. R. Magnus and H. Neudecker, *Matrix differential calculus with applications in statistics and econometrics*. John Wiley & Sons, 2019.
- [37] M. Lanchares and W. M. Haddad, "Stochastic thermodynamics: Dissipativity, accumulativity, energy storage and entropy production," *Philos. Trans. of the Royal Soc. A*, vol. 381, no. 2256, p. 20220284, 2023.
- [38] P. Billingsley, *Probability and measure*. John Wiley & Sons, 2017.
- [39] H. J. Kushner, *Stochastic stability and control*. ACADEMIC PRESS, INC., 1967.
- [40] P. Kidger and T. Lyons, "Universal approximation with deep narrow networks," in *Conf. Learn. Theory*, pp. 2306–2327, 2020.
- [41] F. L. Lewis, A. Yesildirek, and K. Liu, "Multilayer neural-net robot controller with guaranteed tracking performance," *IEEE Trans. Neural Netw.*, vol. 7, no. 2, pp. 388–399, 1996.
- [42] B. Fan, Q. Yang, S. Jagannathan, and Y. Sun, "Asymptotic tracking controller design for nonlinear systems with guaranteed performance," *IEEE Trans. Cybern.*, vol. 48, no. 7, pp. 2001–2011, 2018.
- [43] Z. Cai, M. S. de Queiroz, and D. M. Dawson, "A sufficiently smooth projection operator," *IEEE Trans. Autom. Control*, vol. 51, pp. 135–139, Jan. 2006.
- [44] R. Penrose, "A generalized inverse for matrices," *Math. Proc. Camb. Philos. Soc.*, vol. 51, no. 3, pp. 406–413, 1955.
- [45] S. Axler, *Linear algebra done right*. Springer Nature, 2024.
- [46] P. Ramachandran, B. Zoph, and Q. V. Le, "Swish: a self-gated activation function," *arXiv preprint arXiv:1710.05941*, vol. 7, no. 1, p. 5, 2017.
- [47] K. He, X. Zhang, S. Ren, and J. Sun, "Delving deep into rectifiers: Surpassing human-level performance on imagenet classification," in *Proc. IEEE Int. Conf. Comput. Vision*, pp. 1026–1034, 2015.
- [48] B. Øksendal and B. Øksendal, *Stochastic differential equations*. Springer, 2003.
- [49] J.-F. Le Gall, *Measure theory, probability, and stochastic processes*. Springer, 2022.



Saiedeh Akbari is a Ph.D. candidate in the department of Mechanical and Aerospace Engineering at University of Florida. Her research focuses on developing adaptive learning-based control strategies for stochastic nonlinear systems. Saiedeh completed her Bachelor of Science in Mechanical Engineering at KN Toosi University of Technology in 2020. During her undergraduate studies, she conducted research on discrete-time sliding mode control for permanent magnet DC motors. She then received her Master of Science in Mechanical Engineering at The University of Alabama in 2023, where she worked on nonlinear adaptive control techniques for hybrid systems, with applications in rehabilitation robotics.



Cristian F. Nino received the B.S. degrees in Mathematics and Mechanical Engineering from the University of Florida, Gainesville, FL, USA. He subsequently earned the M.S. degree in Mechanical Engineering, also from the University of Florida, with a focus on control systems. He is currently pursuing the Ph.D. degree in Mechanical Engineering at the University of Florida under the guidance of Dr. Warren Dixon. Mr. Nino is a recipient of the SMART Scholarship, the NSF Fellowship, and the Machen Florida Opportunity Scholarship. His research interests include robust adaptive nonlinear control, multi-agent target tracking, distributed state estimation, reinforcement learning, Lyapunov-based deep learning, and geometric mechanics and control.



Omkar Sudhir Patil received his Bachelor of Technology (B.Tech.) degree in production and industrial engineering from Indian Institute of Technology (IIT) Delhi in 2018, where he was honored with the BOSS award for his outstanding bachelor's thesis project. In 2019, he joined the Nonlinear Controls and Robotics (NCR) Laboratory at the University of Florida under the guidance of Dr. Warren Dixon to pursue his doctoral studies. Omkar received his Master of Science (M.S.) degree in mechanical engineering in 2022 and Ph.D. in mechanical engineering in 2023 from the University of Florida. During his PhD studies, he was awarded the Graduate Student Research Award for outstanding research. In 2023, he started working as a postdoctoral research associate at NCR Laboratory, University of Florida. His research focuses on the development and application of innovative Lyapunov-based nonlinear, robust, and adaptive control techniques.



Prof. Warren Dixon received his Ph.D. in 2000 from the Department of Electrical and Computer Engineering from Clemson University. He worked as a research staff member and Eugene P. Wigner Fellow at Oak Ridge National Laboratory (ORNL) until 2004, when he joined the University of Florida in the Mechanical and Aerospace Engineering Department. His main research interest has been the development and application of Lyapunov-based control techniques for uncertain nonlinear systems. His work has been recognized by the 2019 IEEE Control

Systems Technology Award, (2017-2018 & 2012-2013) University of Florida College of Engineering Doctoral Dissertation Mentoring Award, 2015 & 2009 American Automatic Control Council (AACC) O. Hugo Schuck (Best Paper) Award, the 2013 Fred Ellersick Award for Best Overall MILCOM Paper, the 2011 American Society of Mechanical Engineers (ASME) Dynamics Systems and Control Division Outstanding Young Investigator Award, the 2006 IEEE Robotics and Automation Society (RAS) Early Academic Career Award, an NSF CAREER Award (2006-2011), the 2004 Department of Energy Outstanding Mentor Award, and the 2001 ORNL Early Career Award for Engineering Achievement. He is an ASME Fellow (2016) and IEEE Fellow (2016), was an IEEE Control Systems Society (CSS) Distinguished Lecturer (2013-2018), served as the Director of Operations for the Executive Committee of the IEEE CSS Board of Governors (BOG) (2012-2015), and served as an elected member of the IEEE CSS BOG (2019-2020). His technical contributions and service to the IEEE CSS were recognized by the IEEE CSS Distinguished Member Award (2020). He was awarded the Air Force Commander's Public Service Award (2016) for his contributions to the U.S. Air Force Science Advisory Board. He is currently or formerly an associate editor for ASME Journal of Dynamic Systems, Measurement and Control, Automatica, IEEE Control Systems, IEEE Transactions on Systems Man and Cybernetics: Part B Cybernetics, and the International Journal of Robust and Nonlinear Control.